

Energy **6**, 281 (1959)]; and J. Nucl. Energy **12A**, 47 (1960).

²⁶J. H. E. Mattauch, W. Thiele, and A. H. Wapstra, Nucl. Phys. **67**, 1 (1965).

²⁷*Nuclear Data Sheets*, compiled by K. Way *et al.* (Printing and Publishing Office, National Academy of Sciences-National Research Council, Washington, D.C.), NRC 60-3-105.

PHYSICAL REVIEW C

VOLUME 5, NUMBER 3

MARCH 1972

Experiments on Parity Nonconservation in Nuclear Forces.

III. Gamma Transitions in ¹⁸⁰Hf, ¹⁵⁹Tb, ¹⁸¹Ta, ²⁰³Tl, and ¹⁸²W[†]

E. D. Lipson, F. Boehm, and J. C. Vanderleeden*

California Institute of Technology, Pasadena, California 91109

(Received 22 October 1971)

We have further studied the parity admixtures in nuclear γ transitions by measuring the circular polarization of γ rays from five nuclei with a technique different from that of our work I and II in this series. The experiments were performed with a forward-scattering rapidly reversing Compton polarimeter and a phase-sensitive detection system. The analyzing efficiency of the Compton polarimeter, including effects of multiple scattering, was determined by Monte Carlo calculations. It was necessary in most experiments to apply corrections for polarized bremsstrahlung associated with β decays. Calculations of bremsstrahlung effects were verified by experiments on ¹⁹⁸Au and ¹⁷⁷Lu. The residual asymmetry of the polarimeter itself was determined by control experiments on ¹⁰³Ru. The values of P_γ obtained were ¹⁸⁰Hf 501 keV, $P_\gamma = (-23 \pm 6) \times 10^{-4}$; ¹⁵⁹Tb 363 keV, $P_\gamma = (-1 \pm 5) \times 10^{-4}$; ²⁰³Tl 279 keV, $P_\gamma = (-0.04 \pm 0.10) \times 10^{-4}$; ¹⁸¹Ta 482 keV, $P_\gamma = (-0.031 \pm 0.025) \times 10^{-4}$; ¹⁸²W 1189 keV, $P_\gamma = (-0.25 \pm 0.40) \times 10^{-4}$. A survey and a discussion of these results is presented.

I. INTRODUCTION

In two prior communications^{1,2} (herein referred to as I and II) results were presented on measurements of the circular polarization of γ rays in ¹⁸¹Ta, ¹⁷⁵Lu, ²⁰³Tl, and ⁷⁵As. The observation of a net circular polarization was reported, supporting the presence of parity-nonconserving (PNC) nuclear forces as predicted by weak-interaction theories of the current-current form. The measurements had been performed with a Compton polarimeter using a technique of integrating the detector current. A specially designed switching pattern was used to suppress effects of drifts such as that due to source decay.

In this paper we report on studies of the nuclei ¹⁵⁹Tb and ¹⁸⁰Hf, a preliminary account of which has been communicated earlier,³ as well as ¹⁸²W. These nuclei were chosen because of the presence of close-lying states of opposite parity which are expected to enhance the parity admixture. For comparison, measurements of the previously reported cases ¹⁸¹Ta and ²⁰³Tl were undertaken.

II. EXPERIMENTAL CONSIDERATIONS

To analyze the γ -ray circular polarization a forward-scattering Compton polarimeter was

built. Just as in I and II, the statistical limitations were surmounted with an integral detection technique. In contrast to our earlier current-integration system, which used a complex switching pattern⁴ at relatively low frequency to suppress drifts, the present system uses ac coupling and fast switching.

A block diagram of the system is given in Fig. 1. A 10-Hz reference sine wave from the lock-in amplifier (LIA) is converted into a square wave in the magnet control unit, controlling the power amplifier which in turn drives the forward-scattering magnet. γ rays reaching the detector after scattering in the magnet produce a detector current, which has dc and ac (10-Hz) components, the latter being a measure of circular polarization. The dc component is retained in the interface and the ac component is passed to the LIA which measures the amplitude of the in-phase 10-Hz component of the signal by synchronous demodulation. The output of the LIA is long-term averaged by means of a bipolar voltage-to-frequency converter and a pair of scalars which are read out every 100 sec onto a magnetic tape.

In Fig. 2 we show the Compton polarimeter. γ rays originating in the source material within the titanium capsule scatter off electrons in the inner region of the magnet and are detected by the coax-

ial lithium-drifted germanium detector. The forward-scattering magnet was assembled from eight rectangular cores wound from a 4-mil tape of grain-oriented silicon iron.⁵ The purpose of this laminated material was to suppress eddy currents and thereby permit fast switching. The magnet was surrounded by magnetic shielding foils in order both to contain the 10-Hz stray field and to help isolate the magnet from the earth's magnetic field.

The precision square wave from the magnet control (Fig. 1) has adjustments for the amplitude and time symmetries in order to eliminate false asymmetries arising from terms quadratic in the magnetization (see below). The bipolar power amplifier is programmed to deliver ± 5 A to the magnet, except during reversal when the output voltage clamps at ± 39 V. As a consequence, the magnetization is reversed linearly in 7.4 msec, and thus possesses a trapezoidal waveform. The magnet current of ± 5 A produces a magnetic field of ± 6.5 Oe and saturation induction of ± 17.5 kG. At saturation the net electron polarization $f = \pm f_0$ with $f_0 = 0.067$.

The asymmetry of the detector current is defined by $A = (I_- - I_+) / (I_- + I_+)$, where I_+ (I_-) is the current when the electron spins in the polarimeter are forward (backward). For convenience we abbreviate the numerator and denominator, $\frac{1}{2}(I_- - I_+) = I_N$, and $\frac{1}{2}(I_- + I_+) = I_D$. Thus I_N and I_D can be identified as the ac and dc components mentioned above.

I_D , which had negligible fluctuations, was measured during the course of each experiment with a differential voltmeter across the load resistor of the detector. In the experiments, I_D ranged from 10 nA to 100 μ A; it was corrected when necessary for leakage and dark currents which amounted together to about 0.5 nA.

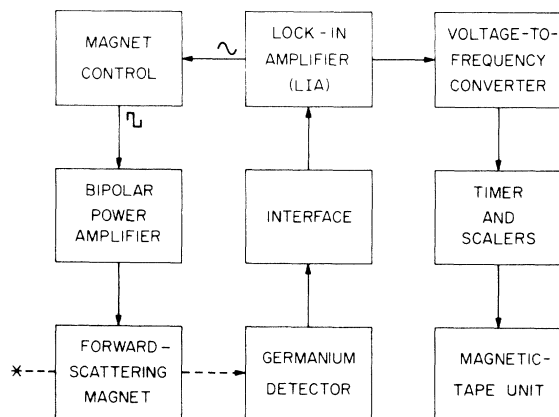


FIG. 1. Block diagram of system.

I_N , buried in noise mainly due to the randomness of the source decay, was separated from I_D by ac coupling and passed to the remote preamplifier of the LIA. The "interface" circuitry between the detector and LIA included detector bias and a filter with passband 1 to 100 Hz.

III. DATA ANALYSIS AND SYSTEMATIC ERRORS

The data were analyzed to allow for source decay, including contributions from radioactive contaminants with various half-lives. $I_N(t)$ and $I_D(t)$ were fitted separately by least squares to determine initial amplitudes for each isotope. Then the asymmetry A could be deduced for the isotope of interest. For a more formal account the reader is referred to Lipson.⁶

Because the asymmetries observed in these experiments were generally $A \leq 10^{-6}$, we were vulnerable to a number of phenomena that could imitate or distort the sought effect. In order to eliminate such "false asymmetries" or in a given case determine their magnitude, we performed a number of control measurements. In I we discussed the sources of experimental error as they applied to that particular apparatus. We now consider in turn the various causes and relative importance of false asymmetries for the present experimental arrangement. Spurious asymmetries arising from source decay, magnetostriction, geomagnetic field, and electromagnetic pickup were all found to be negligible.⁶ In the following we discuss the remaining sources of false asymmetries.

Bremsstrahlung. In all cases except ^{180}Hf the γ -ray transition is fed from a β -decaying parent. The internal and external bremsstrahlung (IB and EB, respectively) following these decays, although weak in intensity is highly circularly polarized and thus contributes to I_N , and to A . In cases where the β end-point energy is not much greater than the γ -ray energy, the bremsstrahlung could be suppressed somewhat by lead filters. Also, the EB could be reduced by diluting the source material with a low- Z material such as carbon. We have calculated IB and EB intensities and polarizations for our cases and checked our calculations with measurements on the β -decaying isotopes ^{177}Lu and ^{198}Au . The method of calculation was basically similar to that described in I, which also contains references to the formulas used. However, for the EB calculations we have introduced a parameter ζ to account, in an average way, for depolarization of the β particles in collisions preceding the creation of the bremsstrahlung quantum under consideration. A reduction factor $1/\zeta$ is applied to the "polarized brems-

strahlung energy spectrum," $P_B(k)kdN_B/dk$, where $P_B(k)$ is the polarization of photons of energy k . The value of ζ is determined experimentally, as discussed in Sec. IV. In Fig. 3 we show the results of our calculations of the IB and EB ($\zeta = 1$) energy spectra and polarizations for ^{198}Au and ^{177}Lu . Calculations were also carried out for ^{159}Tb , ^{181}Ta , and ^{203}Hg , and their results are incorporated in Figs. 4 and 5. For ^{159}Tb and ^{181}Ta where bremsstrahlung was important, the source material was diluted with carbon. Since the EB then contributed only about 15% to the total bremsstrahlung asymmetry, accuracy in the value of ζ was not crucial.

Quadratic effects. These effects arise from the nonlinear polarization dependence of absorption and multiple scattering processes [see second-order term in Eq. (1) below]. They give rise to "false asymmetries" only if the magnetization waveform is asymmetrical in amplitude or time. Thus precise symmetry is required in the magnet current. On the other hand, the quadratic effects do provide an alternative technique for calibrating the system with an unpolarized beam of monochromatic γ rays (as opposed to the continuous spectrum of polarized bremsstrahlung).⁶ The residual

asymmetry from quadratic effects in our experiments was determined to be less than 5×10^{-8} . This was corrected for implicitly by control experiments.

Right-left asymmetry. In a scattering experiment of unpolarized γ rays on polarized iron, Bock⁷ has measured an asymmetry of the form $A = R\vec{s} \cdot \vec{k}_1 \times \vec{k}_2 / |\vec{k}_1 \times \vec{k}_2|$, where \vec{s} is the electron polarization and \vec{k}_1 and \vec{k}_2 are the initial and final photon momenta. Using a rectangular magnet core and a source of ^{103}Ru with γ energy $k = 497$ keV, we verified Bock's early measurements, obtaining $R = (1.7 \pm 0.2) \times 10^{-3}$ at $\theta = 45^\circ$ (resolution $\Delta\theta = 10^\circ$) and $R = (-0.7 \pm 0.1) \times 10^{-3}$ at $\theta = 85^\circ$ ($\Delta\theta = 20^\circ$). More recently Bock⁸ and Lobashov and Smotritskii⁹ have reconsidered these effects and interpreted them as due in large part to double scattering.

In our parity experiment \vec{s} was practically in the plane of \vec{k}_1 and \vec{k}_2 and the asymmetry was thus reduced by orders of magnitude; moreover the noncoplanarities tend to cancel when averaged over the geometry. However, slight misalignments or nonhomogeneities may lead to a nonzero resultant asymmetry for our polarimeter.

With ^{103}Ru sources (497-keV γ ray) and our polarimeter we have observed a net asymmetry A_{Ru}

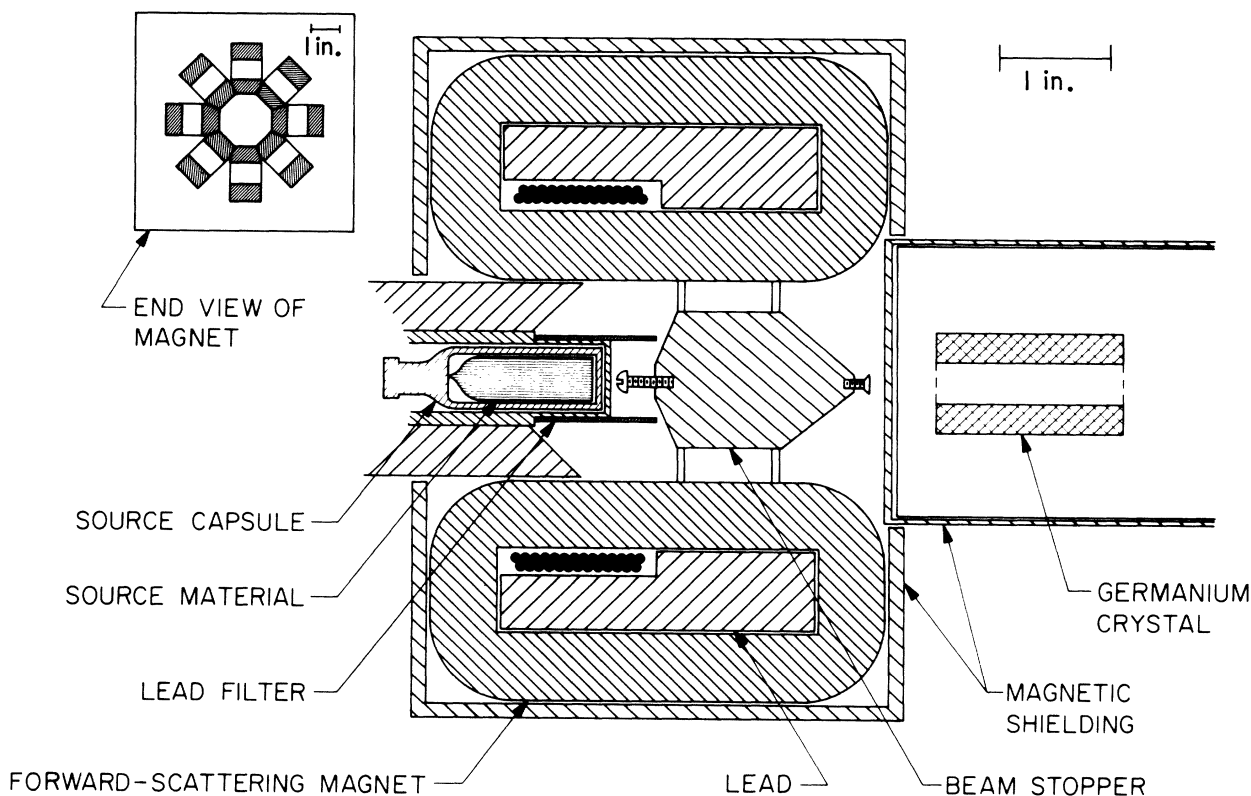


FIG. 2. The Compton polarimeter. Photons from the source are detected in the germanium diode after scattering off electrons in the magnet.

$= (-0.20 \pm 0.03) \times 10^{-6}$ after a small correction for bremsstrahlung, while expecting a negligible contribution from parity effects in this case of a fast $E2$ transition. After additional tests we concluded that this persisting result was due to the right-left asymmetry.

Final data reduction. It remains to deduce the γ -ray polarization from the observed asymmetry A . In general A includes effects from polarized and unpolarized γ rays and from polarized bremsstrahlung. The discrete spectrum is composed of fractions N_i of γ rays with energy k_i and polariza-

tion P_i . To account for attenuations of photons in the source material and capsule we include a factor $S(k)$. We define the polarimeter intensity detection function $D(k) = \langle k_D \rangle / k$, where $\langle k_D \rangle$ is the expectation of the energy deposited in the detector by the resultant scattered photon, assuming initially $P(k) = +1$. We expand $D(k)$ in a power series in f , the net electron polarization in the analyzer,

$$D(k) = D_0(k) + D_1(k)f + D_2(k)f^2 + \dots \quad (1)$$

Then the observed asymmetry is given by

$$A = -f_0 \frac{\sum D_1(k_i)S(k_i)P_i k_i N_i + \int D_1(k)S(k)P_B(k)k(dN_B/dk)dk}{\sum D_0(k_i)S(k_i)k_i N_i + \int D_0(k)S(k)k(dN_B/dk)dk}, \quad (2)$$

neglecting terms of order f^2 . In most cases of interest only one γ ray (say $i = 1$) will have appreciable net polarization. We then write

$$A = A_B + A_\gamma \quad (3)$$

with

$$A_B = -f_0 \frac{\int D_1(k)S(k)P_B(k)k(dN_B/dk)dk}{\text{denom}} \quad (4)$$

and

$$A_\gamma = -f_0 P_\gamma \frac{D_1(k_1)S(k_1)k_1 N_1}{\text{denom}}, \quad (5)$$

where denom is the denominator of Eq. (2) and $P_1 = P_\gamma$ is the polarization of the γ ray. The functions $D_n(k)$ have been evaluated for each value of w , the lead filter thickness, by Monte Carlo calculations¹⁰ including effects of multiple scattering and linear polarization of the γ rays. Given this information, P_γ may be unfolded from Eqs. (2) to (5).

IV. RESULTS

¹⁸⁰Hf. The results for the three series of ¹⁸⁰Hf experiments are summarized in Table I. All Hf sources were irradiated for 5.5 h in a flux of $1.2 \times 10^{14} \text{ cm}^{-2} \text{ sec}^{-1}$ at the General Electric Test Reactor in Pleasanton, California, and the experiments commenced at $t = 6$ –10 h. In the ¹⁸⁰Hf^m sources, there were contaminants of 43-day ¹⁸¹Hf (suppressed somewhat in the enriched sources II and III). These contributed slightly to I_N and more so to I_D at $t \gg 5.5$ h. In addition, there were contaminants from the titanium capsule requiring corrections to both I_N and I_D . Such contaminants were monitored both by γ spectroscopy of the sources and by analysis of $I_D(t)$.

The “numerator” data $I_N(t)$ were fitted as described to determine initial amplitudes $I_N^1(0)$ and $I_N^2(0)$ corresponding to half-lives $T_1 = 5.5$ h (¹⁸⁰Hf^m) and $T_2 = 43$ day. The “denominator” data $I_D(t)$ were fitted for three components $I_D^1(0)$, $I_D^2(0)$, and $I_D^3(0)$ with $T_1 = 5.5$ h, $T_2 = 43$ day, and $T_3 = 40$ h. The value of T_3 was selected by χ^2 tests to accommodate small amounts of capsule contaminants with decay rates in this intermediate range. Two control experiments were performed with capsules (irradiated 5.5 h) containing no Hf powder. Values for this raw asymmetry, $A_{\text{raw}} = I_N^1(0)/I_D^1(0)_{\text{Hf}}$, are given in the second to last column of Table I. Finally we subtract from A_{raw} the asymmetry from the capsule, A_{cap} , yielding A_{final} , given in the last column of Table I.

The presence of a large Na contaminant in the enriched material of series II was established quantitatively by γ spectroscopy. The relative γ intensities indicated the ratio of initial activities of ²⁴Na to ¹⁸⁰Hf^m to be 0.25 ± 0.06 corresponding to about 27 mg Na. We calculated that the ²⁴Na bremsstrahlung contribution would produce an apparent asymmetry of $A_{\text{Na}} = (-8.1 \pm 2.0) \times 10^{-6}$. The corrected final asymmetry is consistent with the other results. The purity of the enriched powder in series III was checked doubly by chemical analysis (flame photometry) and by activation analysis and found to contain < 1 ppm of Na. Furthermore, γ spectroscopy of the sources in all three series established the absence of any other appreciable contaminants.

We considered also the possibility that the observed asymmetry might be due to bremsstrahlung from 4.6-h ¹⁷⁹Lu produced by ¹⁷⁹Hf(n, p)¹⁷⁹Lu in the reactor fast flux. A control experiment with a Hf source irradiated within a cadmium shell (to absorb thermal neutrons and thereby sup-

TABLE I. Results for $^{180}\text{Hf}^m$ experiments. All measurements were performed with a 1-mm lead filter around the source.

Series	Source material isotopic composition ^a		Chemical form	Mass of Hf (g)	Number of experiments	χ^2	Raw asymmetry (units of 10^{-6})	Final asymmetry ^b (units of 10^{-6})
I	14	35	Hf rod	50	1	2.1	-3.5 ± 1.4	-5.1 ± 1.5
			HfO ₂ powder	15	5			
II	75	14	HfO ₂ powder	0.75	5 ^c	4.6	-9.6 ± 1.8	-3.1 ± 2.8 ^d
III	58	30	HfO ₂ powder ^e	1.0	3 ^c	4.8	-2.6 ± 1.8	-3.9 ± 2.0
Mean asymmetry							-4.4 ± 1.1	
Asymmetry referred to 501-keV γ ray (units of 10^{-6}):							-46 ± 11	

^a Isotopic abundance prior to irradiation. Series I used natural abundance material; II and III used enriched material in order to suppress ^{181}Hf .

^b Corrected for ^{103}Ru control $A_{\text{Ru}} = (-0.20 \pm 0.03) \times 10^{-6}$ and for capsule control $A_{\text{cap}} \sim (1.6 \pm 0.5) \times 10^{-6}$.

^c Successive irradiations of one sample.

^d Corrected for effects of ^{24}Na contaminant present in this sample alone: $A_{\text{Na}} = (-8.1 \pm 2.0) \times 10^{-6}$.

^e Diluted 1:3 by mass with carbon powder.

press ^{180}Hf) gave an effective asymmetry [relative to the usual $I_D^1(0)_{\text{Hf}}$] of $A_{\text{Hf}(\text{Cd})} = (+1.4 \pm 2.3) \times 10^{-6}$. This result together with γ spectra of the Hf(Cd) source indicated the absence of ^{179}Lu .

After correction for a small background asymmetry, $A_{\text{Ru}} = (-0.20 \pm 0.03) \times 10^{-6}$ from the ^{103}Ru

control (see above) we find a mean final asymmetry $(-4.4 \pm 1.1) \times 10^{-6}$ [displayed in Fig. 4(a) below the decay scheme] corresponding to a polarization of the 501-keV γ -ray ^{180}Hf given by $P_\gamma = (-2.3 \pm 0.6) \times 10^{-3}$.

¹⁹⁸Au bremsstrahlung control. We chose ^{198}Au

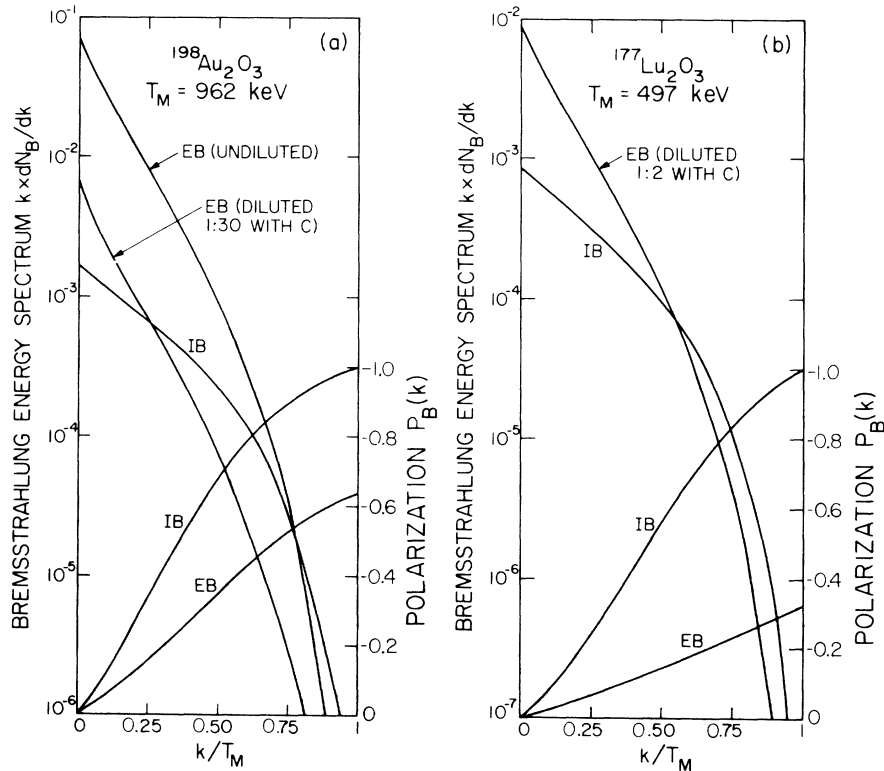


FIG. 3. (a), (b) Internal (IB) and external (EB) bremsstrahlung energy spectra and polarization. T_M denotes the β -decay end-point energy. ($\zeta=1$ in the EB spectra.)

specifically to check the bremsstrahlung asymmetry calculations for ^{159}Gd , because of their similar β end points and γ energies [see decay schemes in Figs. 4(b) and 4(c)]. To this end we prepared a source of 100 mg Au_2O_3 diluted with 3 g C powder, the same composition as the Gd_2O_3 source. In addition we used an undiluted Au_2O_3 source to determine the parameter ζ in our EB calculations. Using these results we calculated the respective asymmetries (referred to the 412-keV γ ray) A_{IB} and $A_{\text{EB}}(\zeta=1)$. Then we evaluated ζ by comparison to the experiments on the undiluted source: $A_{\text{expt}}^{(w)} = A_{\text{IB}}^{(w)} + A_{\text{EB}}^{(w)}(\zeta=1)/\zeta$, with lead thickness $w=0, 1, 2$ mm. This gave $\zeta=1.5$. The fit is shown in the dashed curve and crosses in Fig. 4(b). Using $\zeta=1.5$ for the undiluted source we find very good agreement between calculations and experiment. This gives confidence in our calculations for ^{159}Gd .

^{159}Tb . The Gd source (irradiated three times

for 18 h for three successive experiments) was composed of 100 mg Gd_2O_3 enriched to 92% in ^{158}Gd mixed with 3 g C powder. The dilution served to suppress EB and to provide a large surface-to-volume ratio for the Gd powder to minimize self-shielding effects by ^{155}Gd and ^{157}Gd which have resonances in the thermal-neutron range.

The "numerator" data $I_N(t)$ were fitted with only one component $I_N(0)$ with half-life $T=18.6$ h for ^{159}Gd . Just as with ^{180}Hf we ran an empty capsule control (irradiated for 18 h). The capsule contribution to $I_D(t)$ was considerable here on account of the lower γ intensity from ^{159}Gd . The results were corrected for this capsule asymmetry, which for $t=0$ was found to be $A_{\text{cap}} \approx (-0.3 \pm 1.6) \times 10^{-5}$, and are displayed in Fig. 4(c) and Table II. Subtracting the bremsstrahlung calculations from the data points we obtain the three values for Gd list-

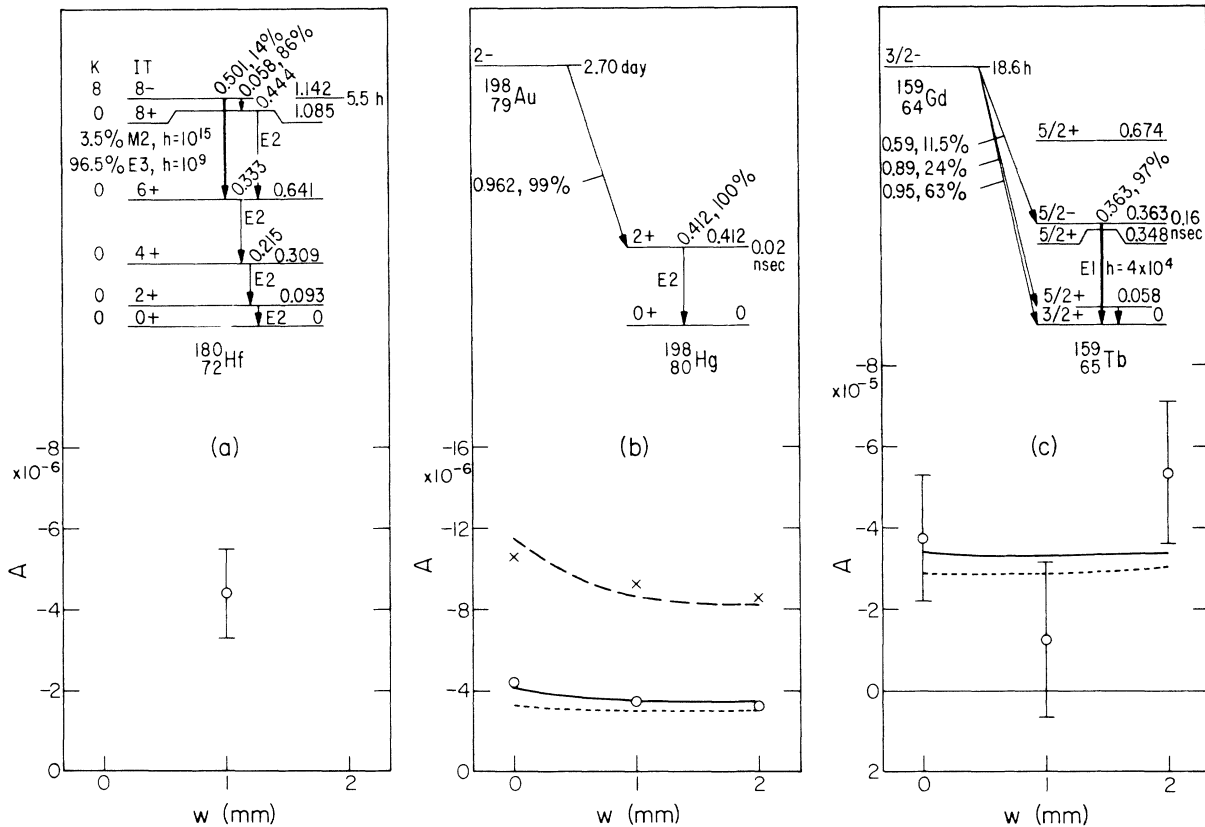


FIG. 4. Asymmetry A vs lead filter thickness w for (a) ^{180}Hf , (b) ^{198}Au , and (c) ^{159}Gd . In (b) and (c) the circles and solid curves are respectively the experiments and total (IB + EB) β bremsstrahlung calculations assuming ($\zeta=1.5$) for sources diluted with carbon. The dotted curves show the IB component alone. In (b) the crosses and dashed curve are the experiments and IB + EB calculations for the undiluted source. The decay schemes shown in (b) and (c) are partial. The hindrance factors h are relative to the Weisskopf estimate. In (b) the errors are about the size of the data points. The bremsstrahlung curves have 5% errors. The asymmetry in (a) is attributed to circular polarization of the 501-keV γ ray. In (c) any net deviation of the data from the solid curve would be attributed to circular polarization of the 363-keV γ ray of ^{159}Tb .

ed in parentheses in Table II. The mean asymmetry for the 363-keV γ ray of ^{159}Tb is found to be $A = (-2 \pm 10) \times 10^{-6}$ corresponding to a circular polarization $P_\gamma = (-1 \pm 5) \times 10^{-4}$.

^{203}Tl . The 100-Ci ^{203}Hg source was prepared by irradiation of 7 g HgO powder for one month at the Experimental Test Reactor (Arco, Idaho). An earlier assembly of the magnet polarimeter was used for the measurement of the ^{203}Tl 279-keV γ transition. A Ru control experiment performed with this magnet gave a right-left asymmetry associated with ^{203}Tl γ rays of $(+0.20 \pm 0.15) \times 10^{-6}$, after corrections for bremsstrahlung and energy dependence of the right-left asymmetry. All Hg runs were performed with zero lead filter thickness ($w=0$), since the bremsstrahlung contribution was minor. In the earlier runs there was a fast decaying ^{198}Au component in I_D and I_N . In the analysis we readily separated the ^{203}Hg component from this short-lived contaminant.

The raw asymmetry for ^{203}Hg was $A_{\text{raw}} = (+0.12 \pm 0.06) \times 10^{-6}$. Subtracting the Ru control and the contribution $A_{\text{brem}} = -0.01 \times 10^{-6}$ (5% error) we obtain the asymmetry listed in Table II. The value A_{Hg} and the curve A_{brem} are shown together with

the decay scheme in Fig. 5(a). Finally, we obtain the circular polarization of the 279-keV γ ray of ^{203}Tl , $P_\gamma = (-4 \pm 10) \times 10^{-6}$.

^{177}Lu bremsstrahlung control. ^{177}Lu was chosen to check the efficiency and bremsstrahlung calculations, in particular for ^{181}Hf . The 100-Ci source was composed of 1 g of Lu_2O_3 mixed with 2 g of carbon powder. The β decays for ^{177}Lu and ^{181}Hf may be compared by inspection of the respective decay schemes in Figs. 5(b) and 5(c). Curves for the spectra and polarization of IB and EB ($\zeta = 1$) are given in Fig. 3 for the 497-keV β branch of ^{177}Lu . The calculated and measured asymmetry results ($\zeta = 1.5$) are shown in Fig. 5(b) and Table II. The good agreement between calculation and experiment supports the bremsstrahlung calculations used for ^{181}Hf .

^{181}Ta . The measurements with a 50-Ci ^{181}Hf source consisting of 0.3 g HfO_2 enriched 98% in ^{180}Hf mixed with 0.6 g carbon were performed with 0- and 2-mm Pb filters. The results, corrected for $A_{\text{Ru}} = (-0.20 \pm 0.03) \times 10^{-6}$ are given in Table II and Fig. 5(c). The circular polarization was found to be $P_\gamma = (-3.1 \pm 2.5) \times 10^{-6}$.

^{182}W . This nucleus for which one might expect a

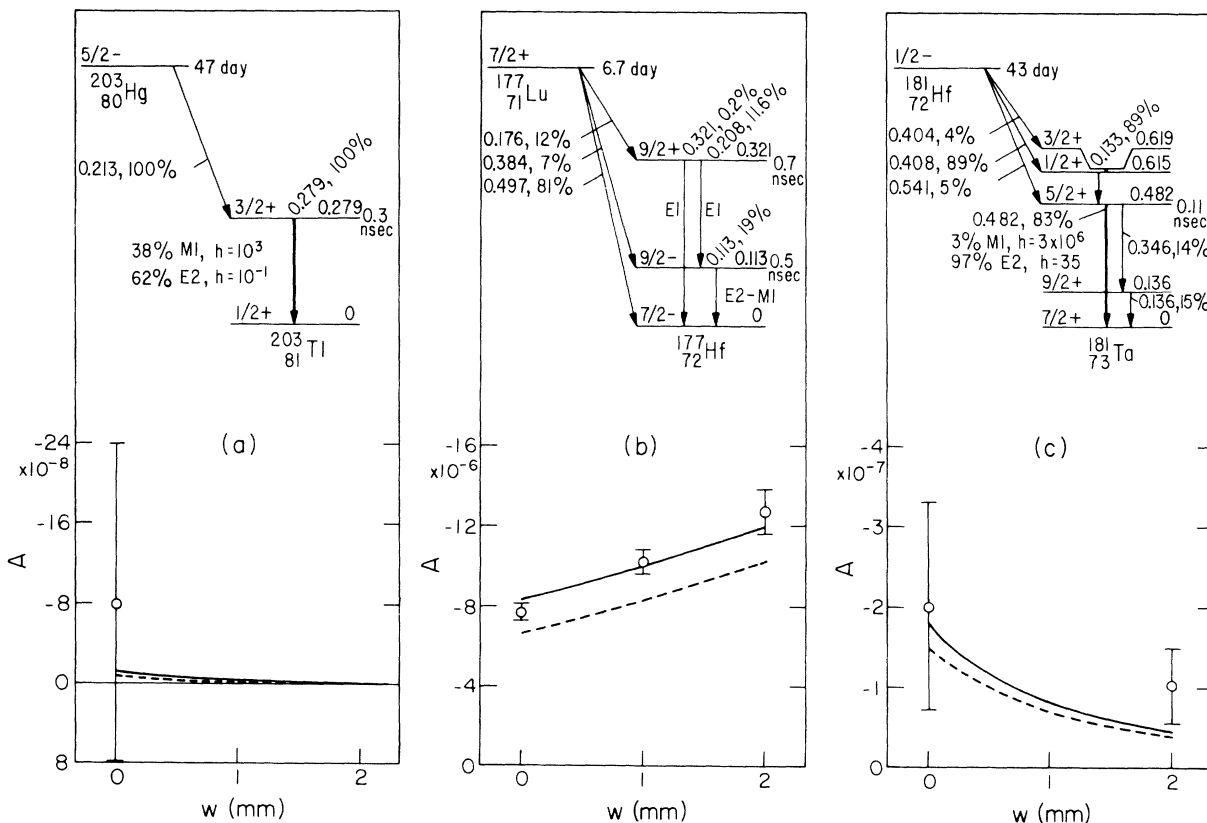


FIG. 5. Asymmetry A vs lead filter thickness w for (a) ^{203}Hg , (b) ^{177}Lu , and (c) ^{181}Hf . For explanation see caption to Fig. 4.

TABLE II. Summary of experimental results.

Isotope	γ -ray energy (keV)	Final asymmetry ^a (units of 10^{-6})			P_γ (units of 10^{-4})
		$w=0$	$w=1$	$w=2$	
^{180}Hf	501	...	-4.4 ± 1.1	...	-23 ± 6
$^{198}\text{Au-Hg}^b$...	(-4.4 ± 0.2)	(-3.5 ± 0.2)	(-3.3 ± 0.2)	...
$^{198}\text{Au-Hg}^c$...	(-10.6 ± 0.3)	(-9.3 ± 0.3)	(-8.6 ± 0.3)	...
$^{159}\text{Gd-Tb}$	363	(-38 ± 16) -4 ± 16	(-13 ± 19) 20 ± 19	(-53 ± 17) -19 ± 17	-1 ± 5
$^{203}\text{Hg-Tl}$	279	(-0.08 ± 0.16) -0.07 ± 0.16	-0.04 ± 0.10
$^{177}\text{Lu-Hg}$...	(-7.7 ± 0.4)	(-10.2 ± 0.6)	(-12.7 ± 1.1)	
$^{181}\text{Hf-Ta}$	482	(-0.20 ± 0.13) 0.02 ± 0.13	...	(-0.10 ± 0.05) -0.06 ± 0.05	-0.031 ± 0.025
$^{182}\text{Ta-W}$	1189	(0.1 ± 0.2) 0.2 ± 0.2	$(-0.33 \pm 0.15)^d$ -0.17 ± 0.15^d		-0.25 ± 0.40

^a Values in parentheses include corrections for zero-asymmetry controls, but not for bremsstrahlung. Values not in parentheses include bremsstrahlung correction. The lead filter thickness (in mm) is denoted by w .

^b Diluted with carbon.

^c Undiluted.

^d Results obtained with apparatus described in I.

TABLE III. Circular polarization of nuclear γ rays, comparison with other experimental results.

Nucleus	γ -ray energy (keV)	P_γ (units of 10^{-4})	Authors
^{180}Hf	501	-23 ± 6	This work
		-28 ± 4.5	Ref. 11
		-18 ± 6	Ref. 13
		-24 ± 3	mean [$\chi_0^2 = 1.8$, $\nu = 2$, $P(\chi^2 > \chi_0^2) = 0.4$]
^{159}Tb	363	-1 ± 5	This work
^{203}Tl	279	-0.04 ± 0.10	This work
		0.02 ± 0.05	Ref. 2
		-0.02 ± 0.3	Ref. 12
		0.03 ± 0.08	Ref. 13
		-0.30 ± 0.18	Ref. 14
		-0.01 ± 0.04	mean [$\chi_0^2 = 3.6$, $\nu = 4$, $P(\chi^2 > \chi_0^2) = 0.5$]
^{181}Ta	482	-0.031 ± 0.025	This work
		-0.06 ± 0.01	Ref. 15
		-0.039 ± 0.012	Ref. 1
		-0.041 ± 0.013	Ref. 16
		0.02 ± 0.04	Ref. 13
		-0.1 ± 0.4	Ref. 12
		$+0.7 \pm 0.7$	Ref. 17
		-0.9 ± 0.6	Ref. 18
		-0.21 ± 0.11	Ref. 19
		-0.28 ± 0.06	Ref. 20
		-0.049 ± 0.006	mean [$\chi_0^2 = 26$, $\nu = 9$, $P(\chi^2 > \chi_0^2) = 0.003$]
^{182}W	1189	-0.25 ± 0.40	This work

large polarization of the 1189-keV γ ray was studied with the present ac system as well as with the dc system described in I. A 20-Ci ^{182}Ta source was produced by neutron irradiation of a 67-g rod of natural abundance Ta. With the present ac system we obtained (for $w = 0$ mm) a raw asymmetry of $A_{\text{raw}} = (-0.19 \pm 0.08) \times 10^{-6}$. This result, corrected for an energy-adjusted right-left asymmetry of $(-0.3 \pm 0.2) \times 10^{-6}$, and for a calculated bremsstrahlung asymmetry of $(-0.09 \pm 0.01) \times 10^{-6}$ leads to $A_{\gamma} = (0.2 \pm 0.2) \times 10^{-6}$ corresponding to a polarization for the 1189-keV γ ray of $P_{\gamma} = (0.8 \pm 0.9) \times 10^{-4}$.

We have also studied the same transition with the apparatus described in I. With the dc system we obtained $A_{\text{raw}} = (-0.31 \pm 0.15) \times 10^{-6}$ for $w = 1$ mm. In this system the right-left asymmetry was found to be $A_{\text{Ru}} = (0.02 \pm 0.03) \times 10^{-6}$. With $A_{\text{brem}} = -0.16 \pm 0.02$ we find $A_{\gamma} = (-0.17 \pm 0.15) \times 10^{-6}$ leading to $P_{\gamma} = (-0.50 \pm 0.44) \times 10^{-4}$. Combining these two independent results we have finally $P_{\gamma} = (-0.25 \pm 0.40) \times 10^{-4}$.

V. DISCUSSION

The results of Sec. III are now compared to values from other experiments and to theoretical estimates. For reference we present in Table III a summary of experiments^{1,2,11-20} measuring P_{γ} for the five nuclei studied here.

^{180}Hf . The 501-keV transition in ^{180}Hf has the largest P_{γ} yet observed in (nonleptonic) parity experiments. Our value $P_{\gamma} = (-2.3 \pm 0.6) \times 10^{-3}$ is in good agreement with the values reported by Jenschke and Bock,¹¹ $P_{\gamma} = (-2.8 \pm 0.45) \times 10^{-3}$, and by Kuphal, Daum, and Kankeleit,¹³ $P_{\gamma} = (-1.8 \pm 0.6) \times 10^{-3}$. The decay scheme is shown in Fig. 4(a). The 501-keV γ ray between the 1142-keV 8^{-} ($K = 8$) isomeric state and the 641-keV 6^{+} ($K = 0$) state has multipolarities $M2$, $E3$, and $\tilde{E}2$ with regular mixing ratio $|\delta| \approx 5.5$. Transitions from the isomeric state to the ground-state rotational band ($K = 0$) are strongly hindered by virtue of their high K forbiddenness.

The unusually large polarization observed here is due presumably to two main features: (a) The amplitude of the irregular $\tilde{E}2$ multipole is enhanced by a factor of 10 compared to the regular $M2$; and (b) in perturbation theory, the closeness of the 8^{-} ($K = 8$) and 8^{+} ($K = 0$) levels (58 keV) enhances the admixture by the PNC force. However, since the PNC potential itself (lacking collective character) would not mix states of different K , we must invoke another mechanism, such as Coriolis (rotation-particle) coupling. Vogel²¹ using such Coriolis mixing in eighth order has estimated $|P_{\gamma}| \leq 2 \times 10^{-3}$. This is in agreement with our observation.

A number of related experiments are possible in ^{180}Hf . The 58-keV transition between the 8^{-} and 8^{+} states should show a comparable polarization. It is more difficult to measure because of its low energy. The present limit for this transition is $|P_{\gamma}| < 5\%$.²² Another possibility is to search for anomalous internal-conversion coefficients for this γ ray; however, the interpretation is complicated by penetration effects.²³ Finally, for the 501-keV γ ray, Krane *et al.*²⁴ have recently reported a large $E3(\tilde{E}2)$ interference in an angular-distribution experiment from oriented nuclei. They find a mixing ratio $|\langle \tilde{E}2 \rangle / \langle M2 \rangle| = 0.038 \pm 0.004$ from which one would derive a circular polarization of $|P_{\gamma}| = (2.6 \pm 0.3) \times 10^{-3}$, in good agreement with our result.

^{159}Tb . ^{159}Tb has similarly to ^{180}Hf an opposite-parity state very near the initial state [see the partial decay scheme shown in Fig. 4(c)]. The $E1$ transition between the 363-keV $\frac{5}{2}, \frac{5}{2}^{-}[532]$ state and the ground-state $\frac{3}{2}, \frac{3}{2}^{+}[411]$ has a hindrance $h = 4 \times 10^4$. The neighboring 348-keV state has quantum numbers $\frac{5}{2}, \frac{5}{2}^{+}[413]$. Admixture of this into the 363-keV state would permit an $\tilde{M}1$ component as well as $\tilde{E}2$. All three multipolarities $E1$, $M1$, and $\tilde{E}2$ are hindered by asymptotic selection rules.

Using Nilsson-model wave functions, Vogel²¹ has estimated P_{γ} for the 363-keV γ ray. He finds that the $\frac{5}{2}^{+}$ 348-keV state gives the dominant contribution to the parity mixing if compared with the two other known $\frac{5}{2}^{+}$ states present. Furthermore, the $\tilde{M}1$ reduced matrix element should exceed the $\tilde{E}2$. Vogel's estimate is $|P_{\gamma}| < 4 \times 10^{-4}$, consistent with our measurement $P_{\gamma} = (-1 \pm 5) \times 10^{-4}$.

In an experiment with nuclei polarized by cryogenic techniques, Krane *et al.*²⁵ have reported an asymmetry $1 + A_1 P_1(\cos\theta)$ in the angular distribution of the 363-keV γ ray. They obtained a value $A_1 = (-1.6 \pm 4.2) \times 10^{-4}$. Assuming $|\langle \tilde{E}2 \rangle / \langle \tilde{M}1 \rangle| \ll 2$, we can write the relationship $A_1 = -1.50 P_{\gamma}$. The observed anisotropy then would correspond to $P_{\gamma} = (+1.1 \pm 2.8) \times 10^{-4}$, in agreement with our result.

^{203}Tl . The partial decay scheme for ^{203}Tl is shown in Fig. 5(a). The 279-keV γ ray has regular multipolarity $M1$, $E2$ ($\delta \approx 1.6$), and irregular multipolarity $\tilde{E}1$. The single-particle (proton-hole) assignments for the initial and final states are $(2d_{3/2})^{-1}$ and $(3s_{1/2})^{-1}$, respectively. Thus the regular $M1$ is hindered ($h = 10^3$) by l forbiddenness. Szymanski²⁶ has estimated for this transition $P_{\gamma} = (-0.9 \pm 0.3) \times 10^{-4}$. More recently McKellar²⁷ predicted $P_{\gamma} = -(0.3 \text{ to } 0.45) \times 10^{-4}$.

In Table III we compare our result $P_{\gamma} = (-0.04 \pm 0.10) \times 10^{-4}$ with four other experimental results. The over-all trend indicates that the theoretical estimates are somewhat high.

^{181}Ta . This transition has been very popular

for such studies (see Table III). The decay scheme is shown in Fig. 5(c). The transition of interest proceeds from the 482-keV $\frac{5}{2}, \frac{5}{2}^+[402]$ state to the $\frac{7}{2}, \frac{7}{2}^+[404]$ ground state. The regular $M1$ is strongly hindered, as indicated on the figure.

An account of the estimates of the circular polarization based on various models is presented in I. More recently, Vinh Mau and Bruneau²⁸ obtained $P_\gamma = -0.8 \times 10^{-6}$, much smaller than previous estimates, and Gari *et al.*²⁹ reconsidering short-range correlations predicted $P_\gamma \approx +0.3 \times 10^{-6}$. Gari and Huffman³⁰ have since demonstrated the need for incorporating interaction current contributions required by gauge invariance. The net effect on the latter value would be to elevate it roughly to the observed value.

In Table III we note the excellent agreement among the first five quoted ¹⁸¹Ta experiments. All of these have achieved small statistical errors by means of integral detection techniques. The

last three experiments listed (which used singles-counting techniques) seem to claim a larger effect but have lower precision. An over-all average is also presented in the table.

¹⁸²W. The 1189-keV transition proceeds from the 1289-keV 2^- state to the 100-keV 2^+ state with regular multipolarity $E1 + 25\% M2$. (For decay scheme see Ref. 31.) Vogel²¹ has considered the contribution of the dominant irregular $E2$ multipole and estimated $|P_\gamma| = 5 \times 10^{-4}$. Recently Krane *et al.*³² have measured the forward-backward asymmetry from cryogenically polarized nuclei for this transition, obtaining a value $W(0^\circ) - W(180^\circ) = (-2.8 \pm 1.7) \times 10^{-4}$. This would correspond to $P_\gamma = (-14 \pm 11) \times 10^{-4}$, which is not inconsistent with our value $P_\gamma = (-0.25 \pm 0.40) \times 10^{-4}$. It would appear from our value of P_γ that any parity mixing in this case lies below the estimate given above.

We wish to thank Dr. P. Vogel for helpful discussions.

†Work performed under the auspices of the U. S. Atomic Energy Commission. Prepared under Contract No. AT-(04-3)-63 for the San Francisco Operations Office, U. S. Atomic Energy Commission.

*Present address: Bell Laboratories, Murray Hill, New Jersey 07974.

¹J. C. Vanderleeden and F. Boehm, Phys. Rev. C **2**, 748 (1970).

²J. C. Vanderleeden, F. Boehm, and E. D. Lipson, Phys. Rev. C **4**, 2218 (1971).

³E. D. Lipson, F. Boehm, and J. C. Vanderleeden, Phys. Letters **35B**, 307 (1971).

⁴J. D. Bowman and J. C. Vanderleeden, Nucl. Instr. Methods **85**, 19 (1970).

⁵Silectron cores from Arnold Engineering Company, Fullerton, California.

⁶E. D. Lipson, Ph.D. thesis, California Institute of Technology, 1971 (unpublished).

⁷P. Bock, Phys. Letters **30B**, 628 (1969).

⁸P. Bock, Lettere Nuovo Cimento **1**, 157 (1971).

⁹V. M. Lobashov and L. M. Smotriskii, to be published.

¹⁰E. D. Lipson and J. C. Vanderleeden, to be published.

¹¹B. Jenschke and P. Bock, Phys. Letters **31B**, 65 (1970).

¹²F. Boehm and E. Kankeleit, Nucl. Phys. **A109**, 457 (1968).

¹³E. Kuphal, M. Daum, and E. Kankeleit, private communication.

¹⁴P. De Saintignon and M. Chabre, Phys. Letters **33B**, 463 (1970).

¹⁵V. M. Lobashov, V. A. Nazarenko, L. F. Saenko, L. M. Smotrisky, and G. I. Kharkevitch, Phys. Letters **25B**, 104 (1967).

¹⁶P. Bock and B. Jenschke, Nucl. Phys. **A160**, 550 (1971).

¹⁷J. J. van Rooijen, P. Pronk, S. U. Ottevangers, and J. Block, Physica **37**, 32 (1967).

¹⁸D. W. Cruse and W. D. Hamilton, Nucl. Phys. **125**, 241 (1969).

¹⁹P. De Saintignon, J. J. Lucas, J. B. Viano, M. Chabre, and P. Depommier, Nucl. Phys. **A160**, 53 (1971).

²⁰E. Bodenstedt, L. Ley, H. O. Schlenz, and U. Wehman, Phys. Letters **29B**, 165 (1969).

²¹P. Vogel, California Institute of Technology Report No. CALT-63-155, 1971 (unpublished).

²²P. Bock, B. Jenschke, and H. Schopper, Phys. Letters **22**, 316 (1966).

²³R. Hager and E. Seltzer, Phys. Letters **20**, 180 (1966).

²⁴K. S. Krane, C. E. Olsen, J. R. Sites, and W. A. Steyert, Phys. Rev. Letters **26**, 1579 (1971).

²⁵K. S. Krane, C. E. Olsen, J. R. Sites, and W. A. Steyert, Phys. Rev. C **4**, 1942 (1971).

²⁶Z. Szymanski, Nucl. Phys. **76**, 539 (1966).

²⁷B. H. J. McKellar, Phys. Rev. Letters **20**, 1542 (1968).

²⁸N. Vinh Mau and A. M. Bruneau, Phys. Letters **29B**, 408 (1969).

²⁹M. Gari, O. Dumitrescu, J. G. Zabolitzky, and H. Kümmel, Phys. Letters **35B**, 19 (1971).

³⁰M. Gari and A. H. Huffman, Phys. Letters **36B**, 442 (1971).

³¹Nuclear Data Sheets, compiled by K. Way *et al.* (Printing and Publishing Office, National Academy of Sciences - National Research Council, Washington 25, D. C.), p. 2110.

³²K. S. Krane, J. R. Sites, and W. A. Steyert, private communication.